Broadband Printed Dipole Antenna with Integrated Balun and Tuning Element for DTV Application

M.H. Teimouri[a],_, Ch. Ghobadi[a], J. Nourinia[a], K. Kaboutari[b], M. Shokri[a], B.S. Virdee[c]

[a]Department of Electrical Engineering, Urmia University, Urmia, Iran
[b]Department of Electronics, Telecommunications and Informatics, University of Aveiro, Aveiro, Portugal
[c]Center for Communications Technology, School of Computing & Digital Media, London Metropolitan University, London N7 8DB, UK

Abstract

This paper presents the design of a broadband printed dipole antenna with an integrated balun and tuning element for DTV applications. Proposed is a unique tuning mechanism that straddled between the gap of the proposed dipole antenna. This enables frequency range of the dipole antenna to be adjusted to tightly cover the specified Digital TV band and thereby mitigating interference from signals outside the band that would otherwise degrade the quality of DTV signal. The measured results confirm the proposed antenna covers an impedance bandwidth of 414.5 MHz from 457.7 to 872.2 MHz, which covers the frequency band of DTV systems (470-862 MHz). Furthermore, the proposed antenna has excellent omnidirectional radiation with a maximum realized gain of 2.95 dBi. These results demonstrate the suitability of the antenna for DTV applications.

Keywords: Digital Television (DTV) Broadband Antenna Integrated Balun Printed Dipole, Tuning Element.

1 Introduction

One of the significant developments facing television media is the transition from analog to digital technologies. In recent decades, most TVs have been analog TVs [1]. Analog systems transmit modulated analog carrier signals from terrestrial broadcasting stations. The only equipment needed to receive such signals is a suitable standard antenna. The number of available TV channels in such systems is limited, and the only available service on them is Teletext. Today, Digital Television (DTV) broadcasting is rapidly being replaced by the traditional analog methods

[2]. Moreover DTV system is becoming very attractive for applications in wireless mobile devices such as laptop computers and vehicles. There are several ways to broadcast digitally to the home. Digital Video Broadcasting, also known as DVB, has a wide variety of operating methods. The Digital Video Broadcasting - Terrestrial (DVB-T) is the DVB European-based consortium standard for the broadcast transmission of digital terrestrial television. DVB-T system transmits compressed digital audio, video, and other data in a MPEG transport stream using Coded Orthogonal Frequency-Division Multiplexing (COFDM) modulation. The data symbols-based transmission mechanism uses multiple carrier frequencies [3]. Thus, the DVB-T digital receiver in home TVs is an analog-to-digital signal converter, which can receive information only through an antenna. From a technical point of view, DVB antennas should cover the frequency band of 470-862 MHz with linear horizontal or vertical polarization. Therefore, the radiation pattern of these antennas must be omnidirectional to receive the signal from all directions.

In recent years, various designs of DVB antennas have been reported in the literature. For example, in [4], the design of a Log-Periodic Dipole Array (LPDA) antenna is presented. The LPDA antenna is composed of dipoles with different lengths. The number of dipoles and their geometric dimensions affect the performance of LPDA. This antenna is suitable for DVB-T receivers operating in the 470-790 MHz band. The LPDA antenna in [4] has low VSWR and high gain. Although at frequencies above 800 MHz its gain is low it can however filter the LTE800 frequency band to thereby improve the reception quality of the antenna in the DVB-T band. A recent example of another LPDA antenna design is reported in [5]. Investigated in [6] is a planar wideband monopole antenna for wireless telecommunication applications and DTV receivers in the UHF band. This antenna is a modified version of triangular-shaped planar wideband monopole antenna. A slot is inserted in the upper section of the radiation patch of this antenna, and several step cuts are made on its sides to achieve a wideband and high gain performance in its operating band. According to the measured results, this antenna covers 450-3060 MHz frequency band with an average gain of 4.62 dBi. In [7], a printed monopole antenna features a technique of increasing its frequency band and reducing its physical size. This antenna can be used in DVB systems operating in the frequency range of 530-860 MHz. The antenna also covers GSM850, GSM900, DCS, PCS, and UMTS frequency bands. Other antenna studies for DVB applications can be found in references [8-12].

Using metal plates [13] or/and dielectric substrates [14-17] are the most commonly used techniques in the design and construction of antennas. Using substrates in antenna design leads to realizing a lightweight, compact, and low-cost antenna [18, 19]. A critical issue faced in the design of antennas is the ability to adjust its frequency band to occupy the specified frequency range. Otherwise the antennas are prone to receive spurious signals that can interefence with the receiver and compromise the quality of system. This can be avoided by employing tuning mechanism in the architecture of the antenna as described in [20]. The tuning element in [20] was used to eliminate unwanted resonant modes to realize wideband performance by locating the tuning element on the backside of the substrate.

This paper presents a novel printed dipole with an integrated balun and tuning element for DTV application. Unlike other tuning elements reported in literature the proposed tuning mechanism is straddled between the gap of the dipole structure. This unique technique enables the operational band of the antenna to be tightly controlled so that it only covers the specified digital TV band and consequently avoid potential signal interference from other wireless systems. Measured results confirm the proposed antenna covers the operating frequency band of 470-862 MHz for DVB systems. Moreover, it has a stable and omnidirectional radiation pattern and an average gain of 2.3 dBi.

2 Antenna Design

Figure 1 shows the configuration of the proposed dipole antenna. The origin of this antenna stem from the conventional half-wave dipole, which consists of two half-wavelength long open-circuited transmission lines in a horizontal configuration and excited by a common source. The size of this type of antenna is too long and its bandwidth is restricted typically between 5-15% of the center frequency. To reduce the size of the dipole antenna and enhance its bandwidth we have proposed the microstrip based dipole structure in Figure 1. The length of each loop-shaped dipole arms is $2 \times (L9 + W1) \approx 0.5\lambda_g$, where λ_g is the guided wavelength at the center frequency of the design. Also, the dipole antenna proposed here is excited inductively using a Γ-shaped feed from below through a slot line as the integrated balun. It was also necessary to include a tuning element, which is a rectangular-shaped stub located under the dipole antenna. The design dimensions in guided wavelength are given in Table 1. The antenna is printed on an FR-4 substrate with a thickness, relative permittivity, and loss tangent of 1.6 mm, 4.4, and 0.02, respectively. A coaxial cable feeds the antenna.

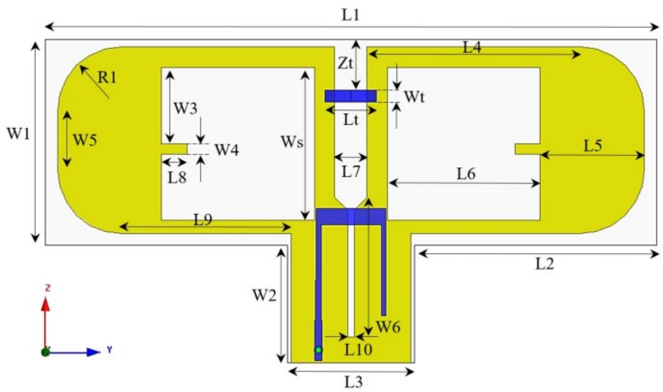

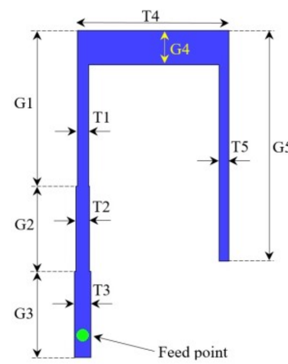

(a) Proposed antenna & dimensional parameters. (b) Geometry & dimensional parameters of the Γ-shaped feed.

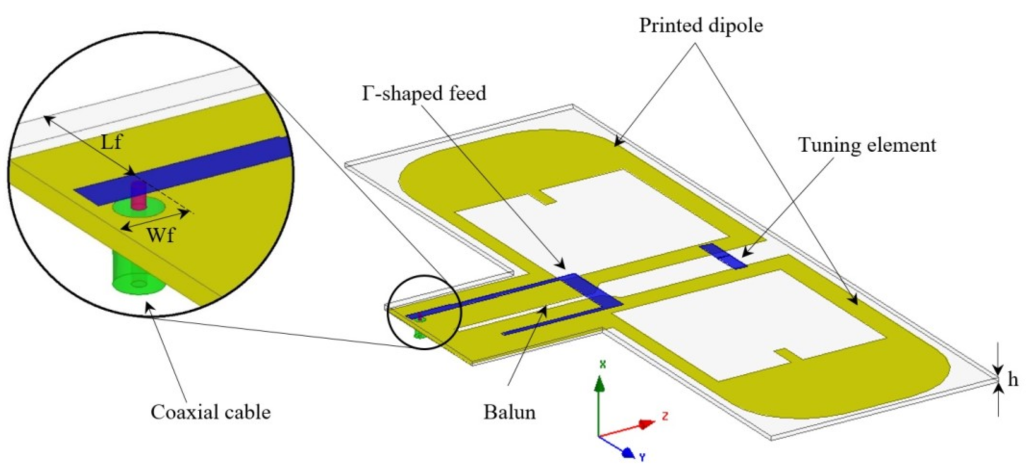

(c) 3D view of the antenna structure and its coaxial cable feed.

Figure 1: Schematic of the proposed dipole antenna.

As will be observed later, the proposed printed dipole antenna with integrated balun is a solution for wideband applications with stable radiation patterns, making it suitable for many wireless systems. Examples of printed dipole antennas with combined balun have inspired the antenna design of Wong and Luk, reported in 2006, who introduced a new kind of complementary antenna referred to commonly as magneto-electric (ME) dipole [21].

The balun design in this article acts like a $\lambda/4$ coaxial balun, which converts the unbalanced coaxial line to a balanced slot line feeding the dipole arms. Two U-shaped slots are etched on the dipole arms to realize the required frequency band, and a tapered Γ-shaped feed structure is used to enhance the input impedance matching of the proposed antenna. The three parts of the Γ-shaped feed are constituted by the microstrip line, the coupling structure, and an open-ended microstrip line. The first part feeds the input power from a coaxial cable to the microstrip line. The coupling structure cooperates with the slot line to hand over the signal to the loop-shaped dipole. Finally, an open-ended microstrip line in the last portion of the feed line faciliates impedance matching. The dimensions of the proposed antenna to cover the DVB operating frequency band are given in Table 1.

Table 1: Design dimensions of the proposed dipole antenna.

Parameters	Dimensions (mm)	Dimensions (λ_g)*	Parameters	Dimensions (mm)	Dimensions (λ_g)*	Parameters	Dimensions (mm)	Dimensions (λ_g)*	Parameters	Dimensions (mm)	Dimensions (λ_g)*
L1	249	0.429	*L2*	95	0.164	*L3*	50	0.086	*L4*	84	0.145
L5	41	0.071	*L6*	60	0.104	*L7*	12.6	0.022	*L8*	10	0.018
L9	66	0.114	*L10*	2.6	0.005	*Lt*	18.8	0.033	*Lf*	12	0.021
W1	80	0.138	*W2*	46	0.08	*W3*	30	0.052	*W4*	4	0.007
W5	23	0.04	*W6*	55	0.095	*Wf*	5	0.009	*W8*	60	0.104
Wt	4.5	0.008	*h*	1.6	0.003	*Zt*	19.9	0.035	*R1*	25	0.043
T1	2	0.004	*G1*	28	0.049	*T2*	2.5	0.005	*G2*	16	0.028
T3	3	0.006	*G3*	16	0.028	*T4*	27	0.047	*G4*	6	0.011
T5	1.8	0.004	*G5*	42	0.073						

*λ_g is guided-wavelength of the antenna's center frequency.

As mentioned above the two radiating elements of a conventional open-circuited transmission line dipole antenna is half-wavelength long. In the investigation here the evolution of the final dipole antenna design is depicted in Figure 2. The design began by employing two interconnected patch antennas. The corresponding reflection coefficient response for each step are shown in Figure 3. The simulation was done using HFSS, a 3D electromagnetic full-wave solver. In step-1 the length of the periphery of the patch antenna is approximately half-wavelength at the center frequency of the design. The antenna was excited from below using a Γ-shaped feed. In step-2, it was discovered that the impedance bandwidth in Figure 3 is improved by reducing the electromagnetic coupling between the dipole arms by widening the gap between them, and by rounding the outer corners of the patch. In step-3, it was discovered that by incorporating a slot in the patch actually improved the antenna's reflection-coefficient response. The rectangular stubs in the slots facilitated fine tuning of the impedance bandwidth. In step-4, it was discovered that by locating an open-circuited stub between the two radiating elements can finely control the coupling between the radiating elements that improved the reflection coefficient of the dipole antenna however this was at the expense of the bandwidth. In our case this was not an issue as the desired DTV's bandwidth (470-862 MHz) was unaffected.

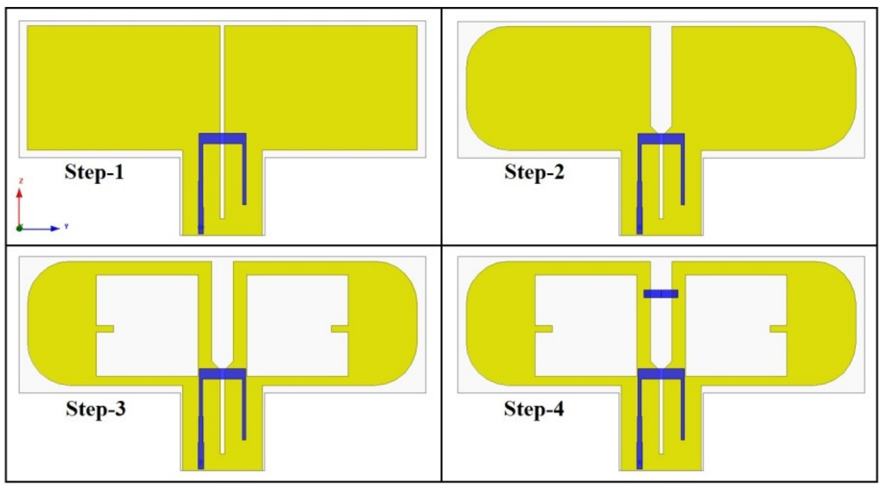

Figure 2: Evolution steps taken in the design of the proposed dipole antenna.

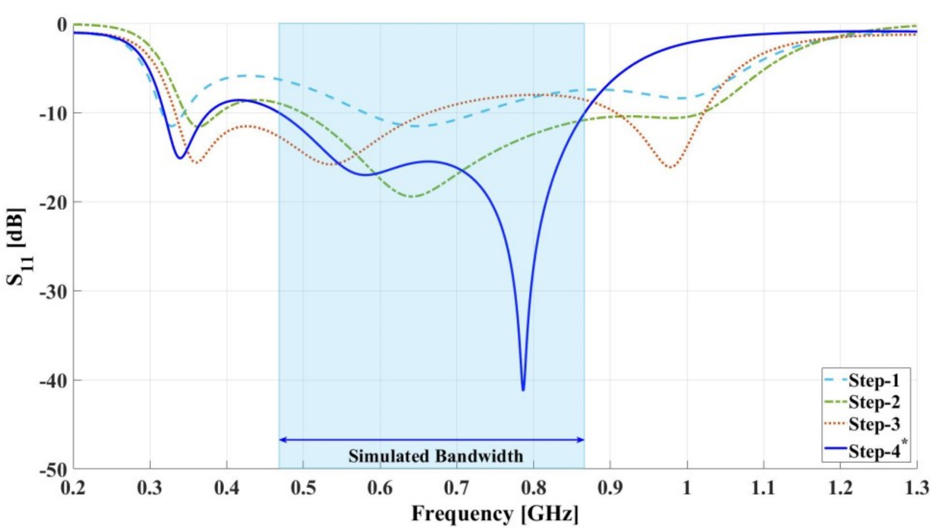

Figure 3: Reflection coefficient response corresponding to each of the four design steps..

The simplified equivalent lumped element circuit of the proposed dipole antenna, shown in Figure 4(a), provides an insight of the parameters that affect the antenna's performance. The equivalent circuit model shows the interaction between the rectangular-shaped tuning element and the dipole that is utilized here to alter the antenna's operating frequency range. The equivalent circuit components, i.e., C_t, L_t and R_t represent the tuning stub, R_d, L_d, and C_d represent the dipoles, and R_f, C_f, and L_f represent the Γ-shaped feed line. The final values of the equivalent circuit are shown in Figure 4(a). The simulated response of the optimised equivalent circuit in Figure 4(b) shows that it's reflection coefficient is better than -10 dB over the DTV spectrum (470-862 MHz). As the lumped element equivalent circuit is a simplified model of the distributed microstrip transmission line based dipole antenna and the results obtained are indicative of the antenna's reflection coefficient response. The simulation was done using Advance Design System by Keysight Technologies.

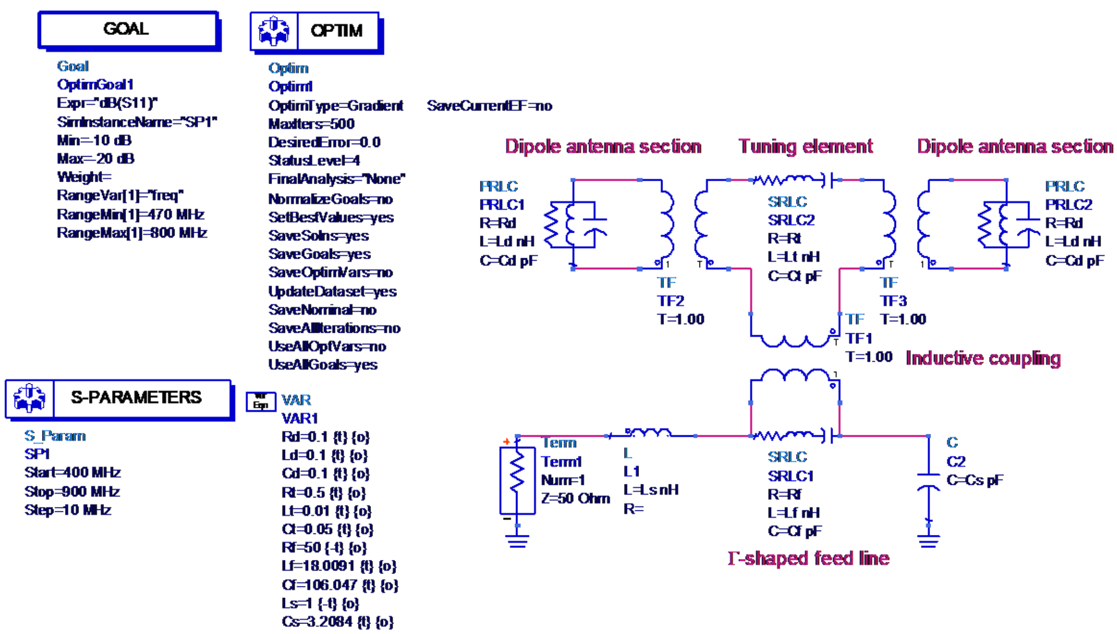

(a)

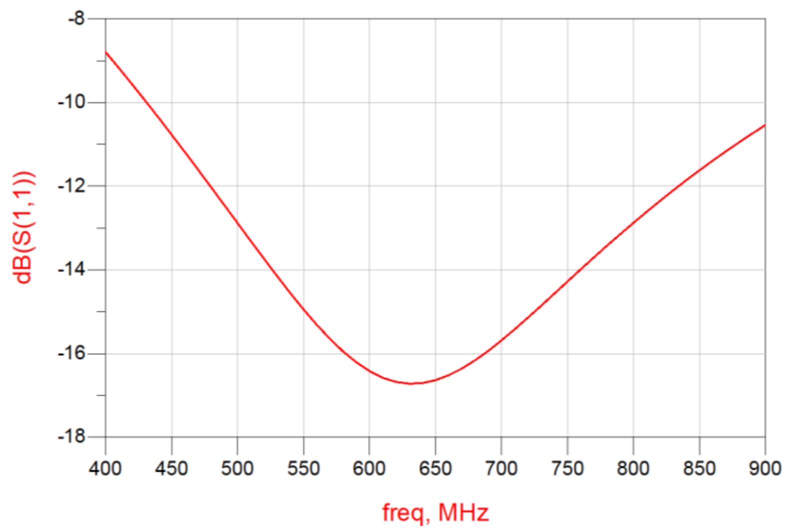

(b)

Figure 4: (a) Simplified equivalent lumped element model of the proposed dipole antenna, and (b) the reflection coefficient response of the optimised circuit.

3 Results and Discussions

HFSS was used to optimize the antenna design. The antenna structure was parameterized in order to study the behavior of antenna's performance using HFSS's optimization facility. Details on the optimization process can be found in these references [22]. Surface currents over the antenna are induced by strong electromagnetic fields and is a function of the frequency. An example of the current distribution at 800 MHz is shown in Figure 5. The surface current distribution is more intense over the Γ-shaped feed the edges of dipole arms, and on the tuning element. This is not surprising as this region is close to the excitation point of the dipoles where the EM-field is more intense. The surface current distribution indicates the key elements at a specified frequency, which is in this case at 800 MHz are L_t, W_t, Z_t, and L_7, that influence the antenna's performance.

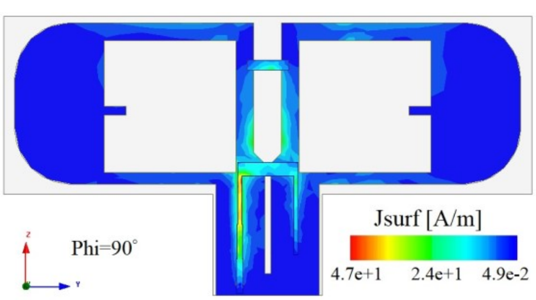

(a) For $\phi = 0°$.

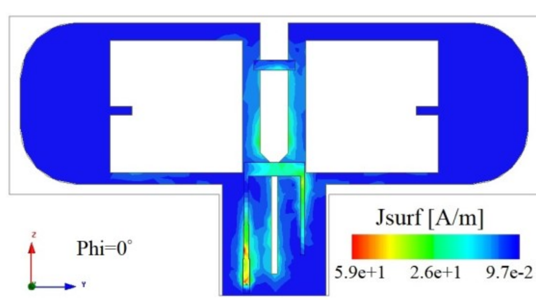

(b) For $\phi = 90°$.

Figure 5: Surface current distribution over the proposed dipole antenna at 800 MHz.

Parametric analysis was performed on the proposed antenna to evaluate how its performance is affected by the tuning element. Figure 6(a) shows that the adjustment of parameter L_7 affects the entire impedance bandwidth of the antenna. From the figure, the L_7 value of 16.6 mm provides an optimum impedance bandwidth performance for S_{11} ≤-10 dB. Furthermore, the effect of varying tuning element's length, width, and vertical distance on the antenna performance is shown in Figures 6(a)-(d). According to these simulated results, it is evident that the tuning element's dimensions and position mainly affect the antenna's upper band frequency. Consequently, the tuning element's length, width, and vertical distance are set at 18.85 mm, 4.5 mm, and 19.9 mm, respectively, to cover DTV's frequency band from 466.2-865.7 MHz. Figure 6(e) shows the influence of parameter L_5 on the impedance bandwidth of the antenna. It is observed from this figure that the lower end frequency can be marginally controlled by varying this parameter. According to the simulation, L_5 of 41 mm is necessary for the antenna to operate over its intended frequency range for S_{11} ≤-10 dB.

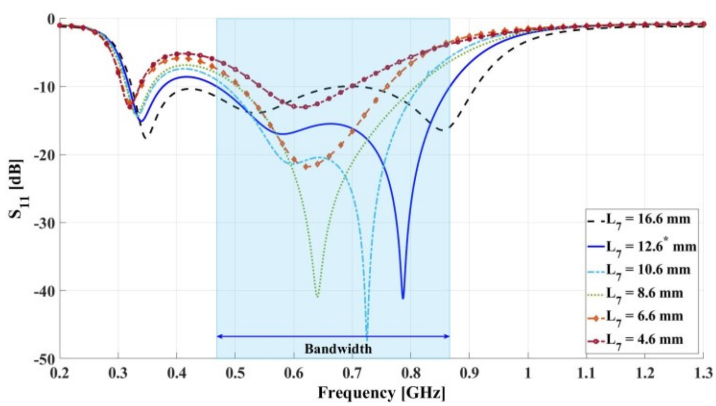

(a) Whole bandwidth of the proposed dipole antenna is controlled by the value of L_7.

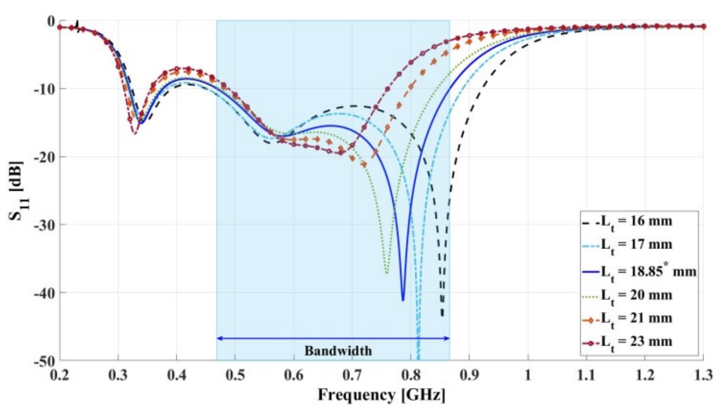

(b) Upper boundary of the proposed dipole antenna's bandwidth is controlled by the value of L_t.

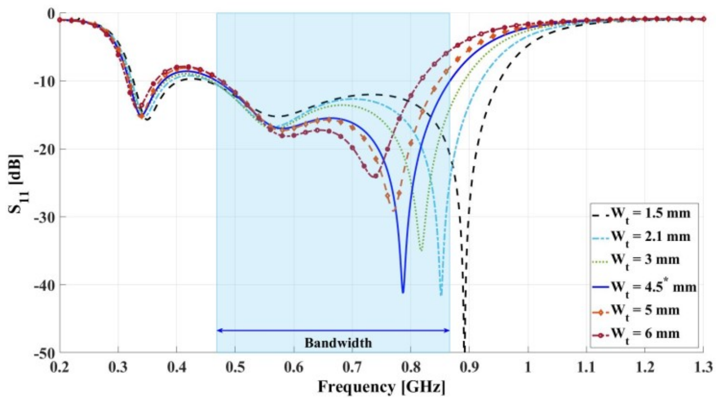

(c) Upper boundary of the proposed dipole antenna's bandwidth is controlled by the value of W_t.

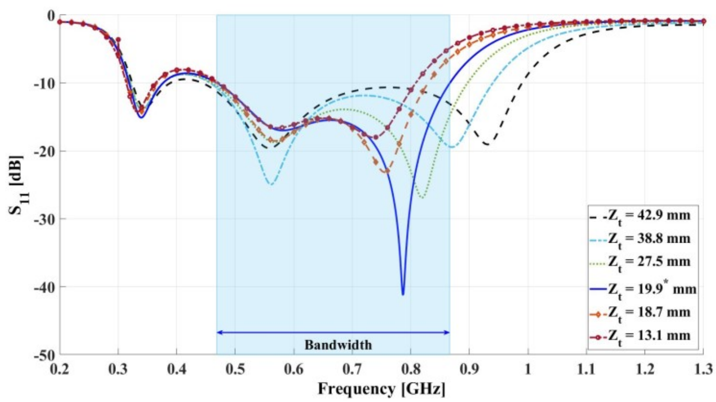

(d) Upper boundary of the proposed dipole antenna's bandwidth is controlled by the value of Z_t.

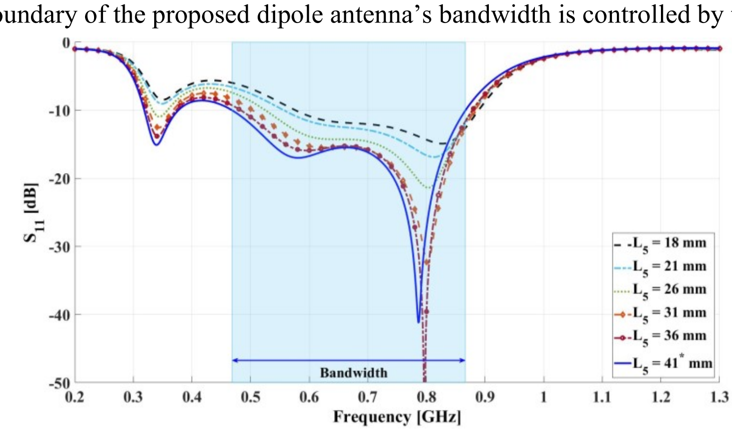

(e) Lower boundary of the proposed dipole antenna's bandwidth is controlled by the value of L_5.

Figure 6: Reflection coefficient responses showing the parameters that control the lower and upper frequency boundary of the proposed antenna's bandwidth.

It can be concluded from the parametric analysis that the upper and lower frequency band edges of the antenna can be precisely controlled. Accordingly, the problem of frequency interference from neighboring wireless systems is mitigated, thereby improving the quality of signal reception by the antenna.

4 Antenna Fabrication and Measured Results

A prototype of the proposed dipole antenna in Figure 1 was fabricated according to the dimensions listed in Table 1. The constructed antenna was tested, and its performance was measured using an Agilent E8363C Network Analyzer. The experimental results were compared with the simulations carried out using HFSS Version 15 x64 software. A comparison of the simulated and measured reflection coefficient responses of the antenna is shown in Figure 7. The results show an excellent correlation between the simulated and measured results, except for a sharp resonant dip at ~0.8 GHz dip and smaller dip between ~0.3-0.4 GHz in the simulated response. The discrepancy reveals inaccuracy in the simulation model.

Based on the simulation results, the proposed antenna has a fractional bandwidth of 59.99% (466.2-865.7) MHz, while the experimental result shows that the fabricated antenna has a fractional bandwidth of 62.34% (457.7-872.2 MHz).

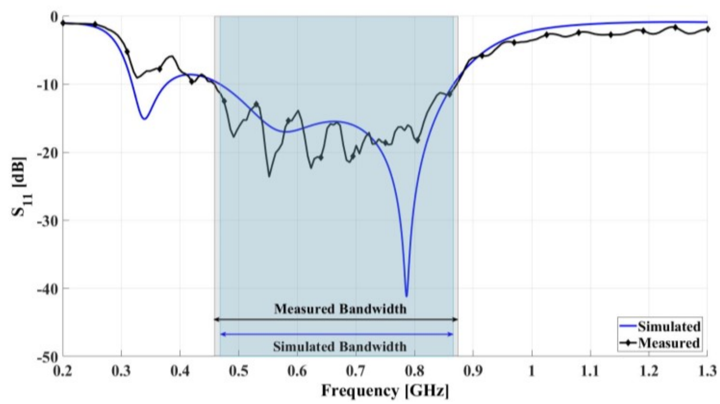

Figure 7: Antenna's measured and simulated reflection coefficient responses.

The proposed dipole antenna's simulated and measured E-plane and H-plane radiation patterns are shown in Figure 8. According to the patterns, the antenna's cross-polarization patterns are at least 20 dB lower than the co-polarization in both orthogonal planes. The antenna radiates omnidirectionally in the H-plane. The experimental and simulation results are in excellent agreement.

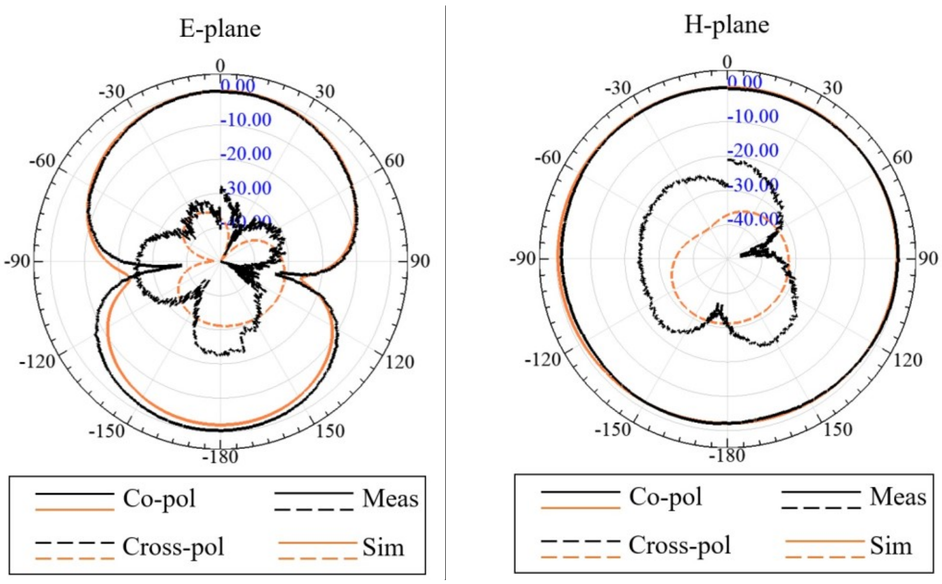

(a) E-Plane radiation pattern. (b) H-Plane radiation pattern.

Figure 8: Simulated and measured E-plane and H-plane radiation patterns of the proposed dipole antenna at 600 MHz.

The simulated and measured realized peak gain of the proposed dipole antenna from 400 to 900 MHz is shown in Figure 9. The highest simulated peak gain at 790 MHz is 3.19 dBi, and the highest measured peak gain of the antenna is 2.95 dBi at 750 MHz. The Axial Ratio (AR) of the proposed antenna, in Figure 10, shows that its polarization is essentially eleptical. Photographs of the fabricated dipole antenna and the measurement setup are shown in Figures 11 and 12.

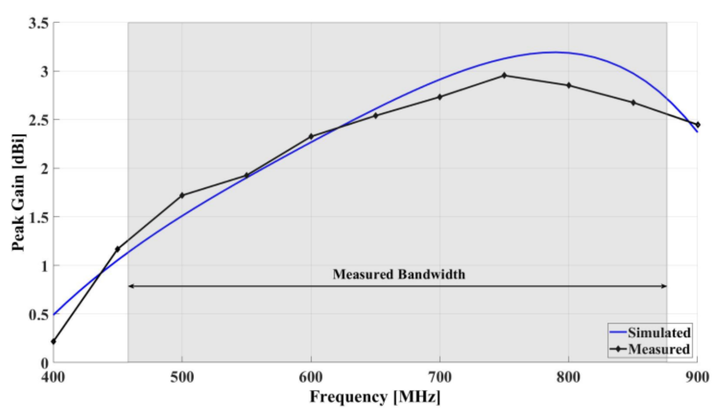

Figure 9: Simulated and measured peak gain of the proposed dipole antenna versus frequency.

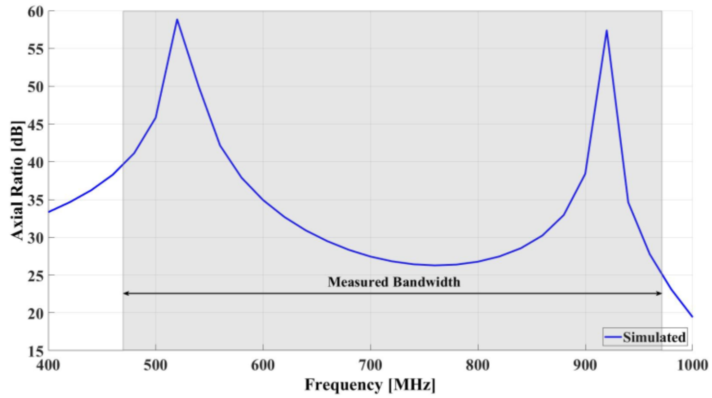

Figure 10: Axial Ratio (AR) of the proposed antenna as a function of frequency.

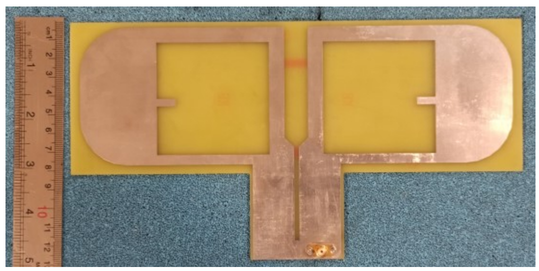

(a) Front-view of the fabricated dipole antenna.

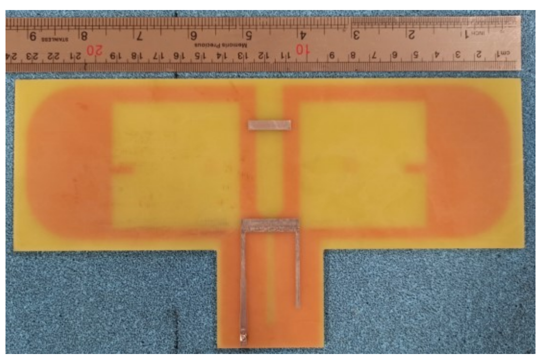

(b) Back-view of the fabricated dipole antenna.

Figure 11: Front and back views of the fabricated dipole antenna.

(a) Antenna reflection coefficient measurement setup using Agilent E8363C VNA.

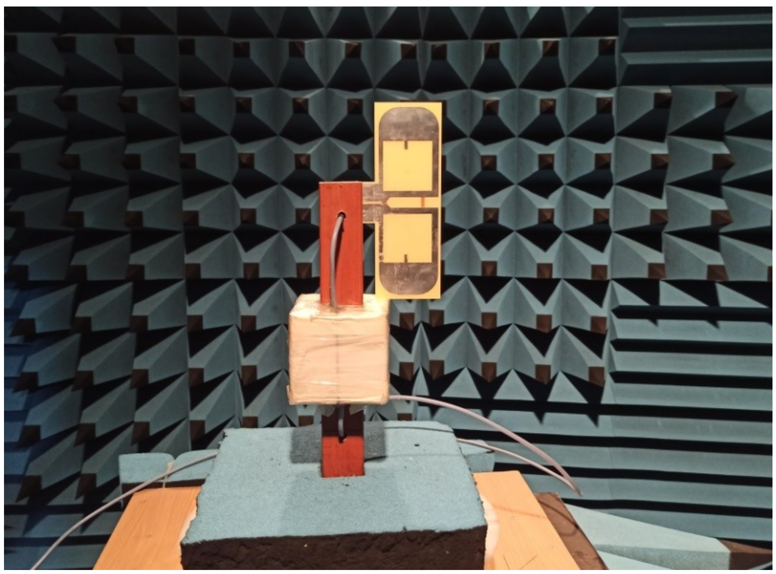

(b) Radiation pattern measurement setup in a standard anechoic chamber.

Figure 12: Setup for measuring the reflection coefficient and radiation patterns of the proposed antenna.

The proposed antenna is compared with other DTV antennas reported in literature in Table 2. The antenna designs in references [6], [7], [23], [24], [26] and [27], in addition to covering the frequency band for digital TV receiver systems also cover frequency bands outside the specified Digital TV band (470-800 MHz) which can cause frequency interference from other transmitters that can degrade the quality of TV signal reception. The operating band of the dipole antenna in [25] falls short for DTV and it has a lower average gain than the proposed antenna. Moreover, unlike the proposed antenna, none of the antennas cited in Table 2 have a feature enabling fine-tuning capability so that only the desired frequency band (470-800 MHz) is covered.

Table 2: Comparison of the proposed dipole antenna with some other DTV antennas.

Ref.	IBW, [MHz]	FBW, %	Size, [mm^3]	Ave. gain, [dBi]	Antenna Type
[6]	450-3060	148.7	172.25×70×1.6	4.62	Monopole
[7]	280-2270	156.1	200×120×1.2	5.57	Monopole
[23]	463-925	66.5	247×160×1.6	2.30	Dipole
[24]	474-1212	87.5	230×35×0.8	1.90	Monopole
[25]	470-771	48.5	210×40×1.2	2.00	Dipole
[26]	589-1000	51.7	200×200×0.8	-	Monopole
[27]	470-860	58.6	80×15×10	-2.25	Monopole
This Work	457.7-872.2	62.3	240×126×1.6	2.95	Dipole

5 Conclusion

A printed dipole antenna with an integrated balun and tuning element is shown to be suitable for DTV application. The coaxial cable-fed antenna with an integrated balun provides excellent impedance matching over the required frequency band. The rectangular-shaped tuning element stub was printed above the Γ-shaped feed structure was used to adjust the antenna's operating frequency to cover the DTV band (470–862 MHz). Measured results confirm that the antenna exhibits a fractional bandwidth of 62.34% (457.7-872.2 MHz) for $S_{11} \leq$-10 dB with an average gain of 2.3 dBi. Moreover, the antenna has a stable and omnidirectional radiation pattern with low cross-polarization.

Acknowledgement

The authors would like to express their special gratitude to the Northwest Antenna and Microwave Research Laboratory (NAMRL) at Urmia University for fabrication and testing the antenna.

References

[1] W. A. L. T. E. R. FISCHER, Digital video and audio broadcasting technology: a practical engineering guide, S.l.: SPRINGER NATURE, (2021) pp. 29–30.

[2] S. O’Leary, Understanding digital terrestrial broadcasting, Boston: Artech House, (2000) pp. 1–15.

[3] P. J. G. D. Hoyo, M. P. J. Amores, D. M. Moya, N. D. R. Maestre, M. R. Zurera, Dvb-t receiver independent of channel allocation, with frequency offset compensation for improving resolution in low cost passive radar,, IEEE Sensors Journal vol. 20, (no. 24) (2020) pp. 14958–14974.

[4] Z. D. Zaharis, I. P. Gravas, P. I. Lazaridis, I. A. Glover, C. S. Antonopoulos, T. D. Xenos, Optimal lte-protected lpda design for dvb-t reception using particle swarm optimization with velocity mutation, IEEE Transactions on Antennas and Propagation, vol. 66, (no. 8) (2018) pp. 3926–3935.

[5] Q. Q. Li, Q. Chu, Y. L. Chang, J. Dong, Tri-objective compact log-periodic dipole array antenna design using moea/d-gpso, IEEE Trans. on Antenna and Propagation, vol. 68, (no. 4) (2020) pp. 2714–2723.

[6] T. H. Kim, Y. Kim, T. H. Yoo, J. G. Yook, Wideband planar monopole antenna for digital tv reception and uhf band communications, IET Microwaves, Antennas and Propagation, vol. 12, (no. 13) (2018) pp. 2041–2045.

[7] E. T. Ashong, Y. B. Jung, Bandwidth enhancement and size reduction of printed monopole antenna using bounding box structure, IET Microwaves, Antennas and Propagation, vol. 13, (no. 9) (2019) pp. 1484–1490.

[8] D. R. Prado, M. Arrebola, M. R. Pino, G. Goussetis, Broadband reflectarray with high polarization purity for 4k and 8k uhdtv dvb-s2, IEEE Access, vol. 8, (2020) pp. 100712–100720.

[9] H. D. Chen, Compact broadband microstrip-line-fed sleeve monopole antenna for dtv application and ground plane effect, IEEE Antennas and Wireless Propagation Letters, vol. 7, (2008) pp. 497–500.

[10] C. C. Hung, C. M. Peng, I. F. Chen, Printed modified bow-tie dipole antenna for dvb/wlan applications, International Journal of Antennas and Propagation, vol. 2013, (2013) pp. 1–6.

[11] J. Machaj, P. Brida, N. Majer, R. Sچ ؤehoviچ ؤ, Impact of gps interference on time synchronization of dvb-t transmitters, Mobile Information Systems, vol. 2021, (2021) pp. 1–11.

[12] A. Desai, R. Patel, T. Upadhyaya, H. Kaushal, V. Dhasarathan, Multiband inverted e and u shaped compact antenna for digital broadcasting, wireless, and sub 6 ghz 5g applications, AEU - International Journal of Electronics and Communications, vol. 123, (2020) pp. 153296.

[13] S. Khorasani, J. Nourinia, C. Ghobadi, M. Shokri, A. Hatamian, B. Virdee, Dual-band magneto-electric dipole antenna with high-gain for base-station applications, AEU - International Journal of Electronics and Communications, vol. 134, (2021) pp. 153696.

[14] K. Kaboutari, V. Hosseini, A compact 4-element printed planar mimo antenna system with isolation enhancement for ism band operation, AEU - International Journal of Electronics and Communications, vol. 134, (2021) pp. 153687.

[15] K. Kaboutari, A. Zabihi, B. Virdee, M. Salmasi, Microstrip patch antenna array with cosecant-squared radiation pattern profile, AEU - International Journal of Electronics and Communications, vol. 106, (2019) pp. 82–88.

[16] M. Shokri, V. Rafii, S. Karamzadeh, Z. Amiri, B. Virdee, Cpw-fed printed uwb antenna with open-loop inverted triangular-shaped slot for wlan band filtering, International Journal of Microwave and Wireless Technologies, vol. 8, (no. 2) (2015) pp. 257–262.

[17] M. Shokri, P. Faeghi, K. Kaboutari, C. Ghobadi, J. Nourinia, Z. Amiri, R. Barzegari, A printed dipole antenna for wlan applications with anti-interference functionality, The 43rd Photonics and Electromagnetics Research Symposium, PIERS, Hangzhou, China, (2021)..

[18] R. Nasirzade, J. Nourinia, C. Ghobadi, M. Shokri, R. Naderali, Broadband printed mimo dipole antenna for 2.4 ghz wlan applications, Journal of Instrumentation, vol. 15, (no. 01), (2020)

[19] A. Eslami, J. Nourinia, C. Ghobadi, M. Shokri, Four-element mimo antenna for x-band applications, International Journal of Microwave and Wireless Technologies, vol. 13, (no. 8) (2021) pp. 859–866.

[20] C. W. Chiu, Y. J. Chi, Printed loop antenna with a u-shaped tuning element for hepta-band laptop applications, IEEE Transactions on Antennas and Propagation, vol. 58, (no. 11) (2010) pp. 3464–3470.

[21] K. M. Luk, H.Wong, A new wideband unidirectional antenna element, Int. J. Microw. Opt. Technol., vol. 1, (no. 1) (Jun. 2006) pp. 35–44.

[22] Optimization of a Dual Band Slot Antenna using ANSYS® HFSS and optiSLang® https://events.prace-ri.eu/event/156/contributions/27/attachments/63/86/Optimierung_Dual_Band_Slot_Antenna.pdf

[23] S. Kornsing, N. Fhafhiem, and A. Innok, Design of wide-band dipole antenna for digital tv broadcasting application, Int. Electrical Engineering Congress (iEECON), (2018), pp. 1-4.

[24] W. S. Chen, J. Jeong, H. T. Chen, J. S. Kuo, Wideband printed monopole antenna for wireless applications, IEEE Antennas and Propagation Society International Symposium, (2009), pp. 1-4.

[25] P. D. Tung and C. W. Jung, Optically transparent wideband dipole and patch external antennas using metal mesh for uhd tv applications, IEEE Transactions on Antennas and Propagation, vol. 68, (no. 3) (2020), pp. 1907-1917.

[26] M. B. Perotoni, M. S. Vieira, S. E. Barbin, and P. A. Garcia, Planar monopole antennas fordigital tv, design, andmeasurement, Microwave and Optical Technology Letters, vol. 56, (no. 3) (2014), pp. 582-586.

[27] J. T. Yeh, W. J. Liao, S. H. Chang, Compact internal antenna for handheld devices with comprehensive dtv band coverage, IEEE Transactions on Antennas and Propagation, vol. 64 (no. 8) (2014), pp. 3998–4007.